International Journal of Advance Engineering and Research Development

VIBRATIONAL SPECTROSCOPIC (FTIR AND FT-RAMAN) STUDIES, UV, NMR AND HOMO LUMO ANALYSIS OF   2-BROMO-1-FLUORO-4-NITROBENZENE

R.Sangeetha [1]   S.Seshadri [2]   Rasheed.M.P [3]

[1]*Research Scholar, PG and Research Department of Physics, Urumudhanalakshmi College,Trichy-19, Tamilnadu, India.*

[2]*Associate Professor and Head, PG and Research Department of Physics, Urumudhanalakshmi College ,Trichy-19,Tamilnadu, India.*

[3]*Research Scholar, PG and Research Department of Physics, Urumudhanalakshmi College,Trichy-19, Tamilnadu, India.*

ABSTRACT-*This work presents the vibrational spectroscopy of 2-Bromo-1-Fluoro-4-Nitrobenzene.The fundamental vibrational frequencies and intensity of vibrational bands were evaluated using density functional theory (DFT) with standard B3LYP/6-311G** method and basis set combinations. The vibrational spectra were interpreted with the aid of normal co-ordinate analysis based on scaled quantum mechanical force field. The infrared and Raman spectra were also predicted from the calculated intensities. Comparison of simulated spectra with the experimental spectra gives essential information about the ability of the computational method to describe the vibrational modes. The ^{13}C and ^{1}H NMR chemical shifts of 2B1F4NB molecules were calculated using the Gauge-Invariant-Atomic Orbital (GIAO).In addition to this, the HOMO, LUMO, chemical hardness(g),chemical potential(I), electrophilicity value(x),total energy and dipole moment are calculated. The molecular electrostatic potential (MESP) is also calculated. The most possible interaction is explained utilizing natural bond orbital (NBO) analysis. The non-linear optical (NLO) property of the title compound has been calculated using first hyperpolarizability components. Thermodynamic properties (heat capacity, entropy and enthalpy of the title compound at different temperatures were calculated. UV-Visible spectrum of the compound was recorded using TD-DFT approach and   Mullikan charges of the molecule were additionally figured utilizing DFT calculations.*

Keywords - 2B1F4NB, DFT, TD-DFT, HOMO, LUMO.

I.INTRODUCTION

Quantum chemical computational methods have proven to be an important tool for interpretations and prediction of vibrational spectra [1, 2].A significant advent in this area was made by the scaled quantum mechanical force field method [3-6].In the SQM approach ,the systematic errors of the computed harmonic force field are corrected by a few scale factors that have been found to be well transferrable between chemically related molecules.[2,7-9].

In our present work, we recorded FTIR and FT-Raman spectrum and calculated the vibrational frequencies of 2B1F4NB in the

ground state to distinguish fundamentals from experimental vibrational frequencies and geometric parameters using DFT/B3LYP (Becke3-Lee-Yang Paar) method. Furthermore, the Gauge invariant–atomic orbital(GIAO) ^{13}C and ^{1}H chemical shifts calculations of the title compound were calculated by using B3LYP/6-311G** basis set.[10]

II. EXPERIMENTAL DETAILS

The fine sample of 2-Bromo-1-Fluoro-4-Nitrobenzene was obtained from Sigma Aldrich, UK, and used as such for the spectral measurements. The room temperature FTIR spectrum of the compound was measured in the 4000–400 cm^{-1} region at a resolution of ±1 cm^{-1}, using a BRUKER IFS-66V vacuum. Fourier transform spectrometer equipped with a Mercury Cadmium Telluride (MCT) detector, a KBr beam splitter and globar source. The FT-Raman spectrum of 2B1F4NB was recorded on a BRUKER IFS–66V model interferometer equipped with an FRA–106 FT-Raman accessory. The spectrum was recorded in the 3500–50 cm^{-1} Stokes region using the 1064 nm line of an Nd: YAG laser for the excitation operating at 200 mw power. The reported wave numbers are expected to be accurate to within ±1 cm^{-1}.

III. COMPUTATIONAL DETAILS

All the calculations were performed by utilizing Gaussian 09 program package on the personal computer. The Becke's three parameter hybrid density functional, B3LYP, was used to calculate both harmonic and anharmonic vibrational

wavenumbers with 6-311G** basis set. It is well known in the quantum chemical literature that the B3LYP functional yields a good description of harmonic vibrational wavenumbers for small and medium sized molecules. The optimized structural parameters were used in the vibrational frequency calculations at the DFT levels to characterize all stationary points as minima. The basis set 6-311++G (d,p) augmented by 'd' polarization functions on heavy atoms and 'p' polarization functions on hydrogen atoms have been used[11,12].

Absolute Raman Intensities and infrared absorption intensities have been calculated with harmonic approximation at the same level of theory as used for optimized geometries from the derivatives of polarizability and dipole moment related with each normal mode. The potential Energy distribution is done to get finish data of the molecular motions involved in the normal mode using MOLVIB program [13]. The experimentally observed spectral data of the compound are found to be in good agreement with the spectral data obtained by quantum chemical calculations. Vibrational wavenumbers calculated have been scaled [14] with the scale factor in order to figure out how the calculated data are in good agreement with those of the experimental ones. Calculated vibrational frequencies have been scaled down by using the scaling factor [14] to offset the systematic error caused by neglecting anharmonicity and electron density.

IV. PREDICTION OF RAMAN INTENSITIES

The Raman activities (Si) calculated with the GAUSSIAN 09 program and adjusted during the scaling procedure with MOLVIB were subsequently converted to relative Raman intensities (Ii) using the following relationship derived from the basic theory of Raman scattering [15,16].

$$I_i = \frac{f(\nu_o - \nu_i)^4 S_i}{\nu_i \left[1 - \exp\left(\frac{-hc\nu_i}{kT} \right) \right]}$$

where ν_0 is the exciting frequency (in cm^{-1} units); ν_i i is the vibrational wave number of the ith normal mode, h, c and k are fundamental constants and f is a suitably chosen common normalization factor for all peaks intensities. Raman activities are reported in **Table.2.**

V. RESULTS AND DISCUSSION

5.1 Optimized Geometry

The numbering framework in the molecular structure of 2B1F4NB is obtained from Gaussian 09W and gaussview 5.0 programs are shown in **Fig.1.**The bond lengths and bond angles are recorded in **Table.1.** utilizing DFT/B3LYP method with 6-311++G(d,p) basis set.
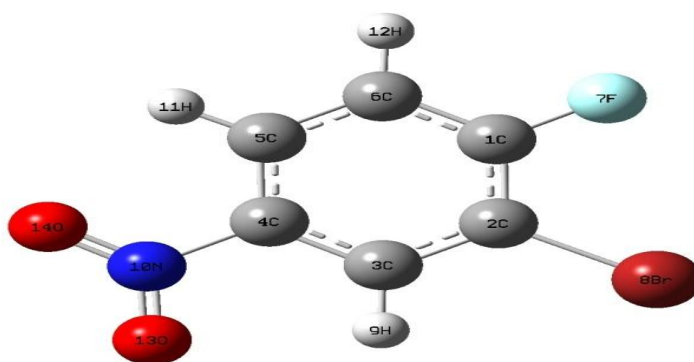

Fig.1.Molecular structure of 2B1F4NB along with numbering of atoms

TABLE 1-*Optimized geometrical parameters of 2B1F4NB obtained by B3LYP/6-311++G(d,p) density functional calculations*

Bond length	Angstrom (Å)	Bond angle	Degree	Torsional angle	Degree
C3-H9	1.080569	C1-C6-C5	119.48	H9-C3-C4-N10	0
C5-H11	1.080703	H9-C3-C4	120.03	H11-C5-C6-C1	-180
C6-H12	1.0825	H11-C5-C6	121.5	H12-C6-C1-C2	-180

				O13-N10-C4-C3	0
O13-N10	1.223572	H12-C6-C5	121.54		
O14-N10	1.223576	O13-N10-C4	117.63	C1-C6-C5-C4	0
C1-C6	1.388888	O14-N10-O13	124.94	C5-C4-C3-C2	0
C3-C2	1.389178	C4-C3-C2	118.72	C6-C5-C4-C3	0
C4-C3	1.390545	C5-C4-C3	122.39	O14-C4-O13-N10	0
C5-C4	1.391123	C6-C5-C4	118.61	F7-C2-C6-C1	0
C6-C5	1.387868	F7-C1-C6	118.64	Br8-C3-C1-C2	0
F7-C1	1.338812	N10-C4-C5	119.07	N10-C3-C5-C4	0
N10-C4	1.478849	Br8-C2-C1	120.2		
Br8-C2	1.899147				

The comparative IR and Raman spectra of experimental and calculated frequencies are given in the **Fig.2** and **Fig.3**
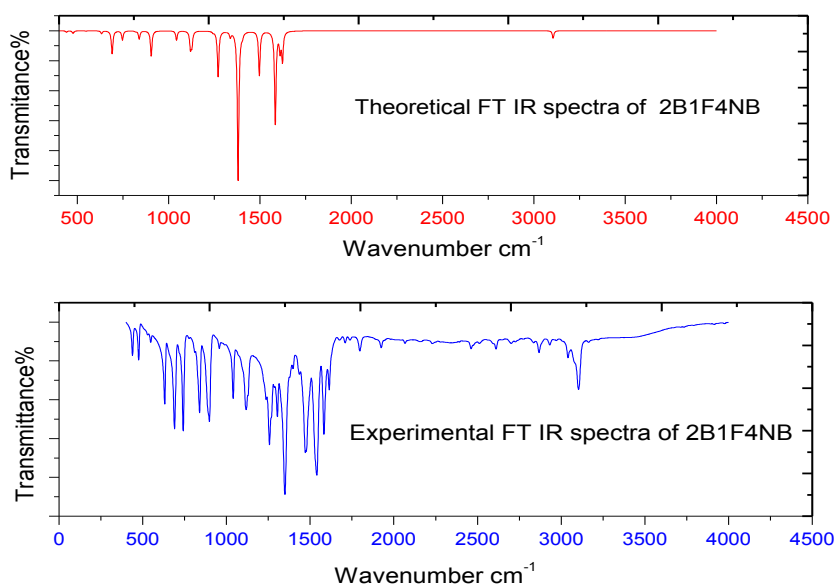

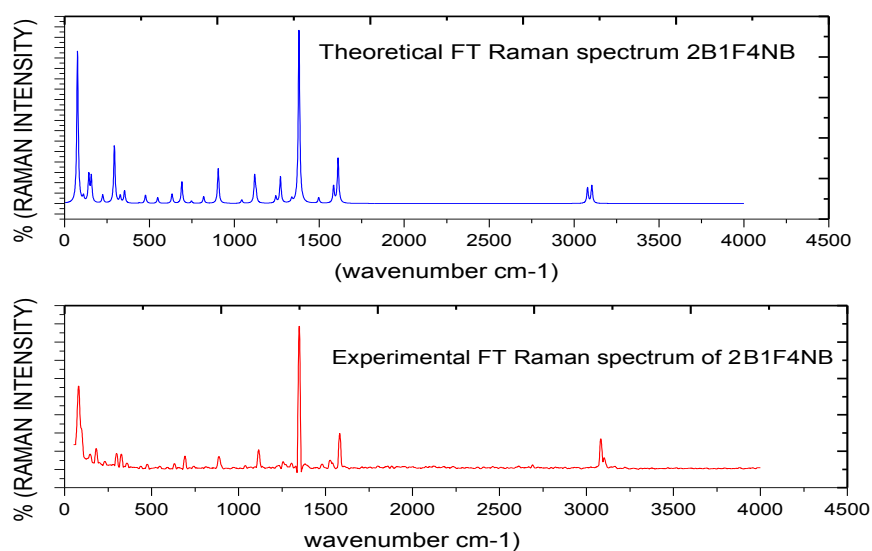*Fig.2. Comparison of Theoretical and experimental FTIR spectrum of 2B1F4NB*

Fig.3. Comparison of Theoretical and experimental FT-Raman spectrum of 2B1F4NB.

5.2.Vibrational Assignment

Infrared and Raman spectra contain various groups at specific wave numbers. The point of the vibrational investigation is to choose which of the vibrational modes give rise to each of these observed bands. The assignments for the key methods of vibrations have been made on the basis of the position, shape and intensity. Vibrational frequencies of comparable compounds like derivatives benzene, pyridine and pyridimine compounds [17, 18] have been taken into consideration for the assignment of fundamental vibrations of 2B1F4NB.

TABLE. 2.Observed and B3lyp /6-311++g(d,p) level calculated vibrational frequencies (in cm^{-1}) of 2-Bromo-1-Fluoro-4Nitrobenzene

No	symmetry species	Observed frequency		Calculated frequency (cm^{-1})with B3LYP/6-311++G(d,p) force field				Characterisation of normal modes with PED%
		IR (cm^{-1})	Raman (cm^{-1})	Unscaled (cm^{-1})	Scaled (cm^{-1})	IR intensity	Raman activity Si	
1	A"	-	80.69	45.48	77	0.0237	1.0849	tNO2(83), tring (12)
2	A"	-	-	113.94	111	4.7136	0.3812	tring(50), tNO2 (36), gCH (11)
3	A'	-	146.86	141.30	143	0.8947	1.243	bCN (50), bCBr (37)
4	A"	-	181.72	151.75	157	0.0012	1.327	tNO2(36), tring (24),gCN(20) gCBr (11)
5	A'	-	231.60	226.99	225	1.784	0.6789	bCF(29),bCBr(29),bCN(17),υCBr(0)
6	A'	-	298.72	295.85	293	1.7398	6.4149	υCBr(36), bring (23),bCN(13) bCBr (10)
7	A"	-	326.12	324.10	327	0.4506	1.1928	tring(43), tNO2 (22),gCH (17)
8	A"	-	358.03	355.84	353	0.2087	1.6082	bring (56),υCN(28)
9	A"	438.76	-	446.03	441	3.7117	0.0303	tring (48), gCBr (33)
10	A'	475.85	474.81	476.22	476	6.1442	2.0078	bCF (53), bCNO(13),υCBr(12), bCBr (10)
11	A"	547.72	-	526.79	480	0.78	0.2253	tring (51), gCN (24),tNO2(15)
12	A'	-	-	553.83	548	1.1302	1.2401	bCNO (45), bCN(17), bCF(12)
13	A'	631.39	631.46	642.05	634	13.4141	2.8231	bring (71), υCN(10)
14	A"	689.76	-	681.73	690	0.1372	0.2876	tring (41), gCF(34), gCBr(14),
15	A"		691.91	698.30	691	46.1979	9.822	bring (36), υCBr (24), υCC(11)
16	A"	741.93	-	723.04	747	18.6336	1.032	tNO2 (66), gCN (18), gCH(10)
17	A'	839.63	-	824.37	823	2.7608	2.5644	bring (41),υCF (16),υCC (15),bONO (13)
18	A"	-	887.29	844.23	839	27.3334	0.0279	gCH(68), gCF(14),tring(12)
19	A"	957.52	-	900.80	904	39.9688	19.73	gCH(80)
20	A'	-	-	921.92	909	21.8836	0.1574	υCC(22),bONO(19),υCN(17), bring (10),
21	A'	--	-	974.22	952	0.0658	0.1067	gCH(92)
22	A'	1040.2	-	1057.83	1043	19.4274	3.3466	bring(40),υCC(25),bCH(17),CBr (11)
23	A'	1117.8	1115.7	1124.07	1118	65.5506	34.229	υCN (27),υ CC(25), bring(20), bCH (19)
24	A'			1142.20	1128	21.1093	4.0657	bCH (70),υ CC(23)
25	A'	1257.0	1256.0	1256.03	1244	18.1688	14.879	bCH (74),υ CC(15)
26	A'		1305.0	1275.62	1271	101.4631	18.147	υCF(46), υCC(23),bCH(23)
27	A'	1349.3		1342.06	1338	23.6154	8.1116	υCC(94)
28	A'		1382.1	1369.42	1382	322.4785	195.97	υNO(67),υCN(17)
29	A'	1436.0		1423.02	1404	2.8937	1.0639	υCC (60),bCH(21)
30	A'	1526.3	1471.3	1503.83	1497	113.2807	4.99	υCC(41), bCH(40),υCF(12)
31	A'	1582.6	1581.7	1584.40	1583	240.0968	24.789	υNO (70), υCC(22)
32	A'	1614,0		1619.55	1611	45.6188	71.069	υCC(69),bring(10)
33	A'		1674.5	1644.16	1623	39.2913	2.7325	υCC (52), υNO(25)
34	A'	-	3082.7	3204.30	3079	0.016	110.20	υCH(99)
35	A'	-	3102.1	3229.7	3104	6.7491	88.488	υCH(99)
36	A'	3103.8	-	3231.32	3106	11.2377	37.197	υCH(99)

5.2.1.C-H stretching

These vibrations show characteristic weak bands in the region 3100-3000cm^{-1}.[19] Three stretching modes have been assigned at 3103 cm^{-1} in FT-IR spectrum 3102 and 3082 cm^{-1} in FT-Raman spectrum for 2B1F4NB. Their calculated values scaled to 3106, 3104 and 3079 cm^{-1} respectively with a PED contribution of 99%.

The C-H in-plane-bending vibrations in aromatic heterocyclic compounds characterized by several medium to strong intensity bands in the region between 1300 and 1000 cm^{-1}. At a point, when there is in-plane interaction over 1200 cm^{-1}, a carbon and its hydrogen usually move in opposite direction [20]. Accordingly for our present sample, the C-H in–plane bending vibrations are observed at 1526,1436,1257,1117 and 1040 cm^{-1} in FTIR spectrum and 1471, 1305, 1256 and 1115 cm^{-1} in FT Raman spectrum is comparatively shifted to higher frequency as its force constant values are high. The theoretically calculated values for C-H in-plane bending vibrations are 1503, 1423, 1256, 1124 cm^{-1}and 1057 cm^{-1}.The experimental and the theoretical values are found to be in good agreement.

The C-H out-of-plane bending vibrations occur in the frequency range 1000 and 650 cm^{-1} [10].The out-of-plane bending modes have established their peaks at 957, 741 cm^{-1} in FTIR spectrum and 887 cm^{-1} in FT Raman spectrum respectively.

5.2.2. C-C Vibrations

The ring carbon–carbon stretching vibrations usually observed in the region 1625-1430 cm^{-1}.For aromatic six membered rings, e.g., benzene and pyridines, there are two (or) three bands in the region due to skeletal vibrations, the strongest usually being at about 1500 cm^{-1}.[22] Therefore, the C-C stretching vibrations of the title compound are found at 1614,1582,1526,1436,1349,1257,1117,1040 and 839 cm^{-1} in FTIR and the FT Raman spectra are found at 1674,1581,1471,1305,1256,1115 and 691 cm^{-1} respectively and these modes are confirmed by their PED values. Most of the ring vibrational modes are affected by the substitutions in the aromatic ring of 2B1F4NB. The reductions in the frequencies of these modes are due to the change in force constant and the vibrations of the functional groups present in the molecule. The theoretically computed values for C-C vibrational modes by B3LYP/6-31+g(d,p) method gives excellent agreement with experimental data.

5.2.3. C-N Vibrations

The identification of C-N vibrations is a very difficult task since mixing of several bands is possible in this region. [23].However with the help of force field calculations, the C-N stretching vibrations are identified and assigned in this work. The FTIR bands appearing at 1117 and 631 cm^{-1} and FT Raman band appearing at 1382, 1115, 631 358 cm^{-1} for 2B1F4NB. The in-plane and out-of-plane bending vibrations assigned for 2B1F4NB are also presented in Table.2. Corresponding bands are theoretically calculated at 1124, 1369, 642 and 355cm^{-1}. Theoretical and Experimental values are found to be in good agreement.

5.2.4.NO$_2$Vibrations

The characteristic group frequencies of the NO$_2$ are independant of the rest of the molecule. Aromatic nitro compounds have strong absorptions due to the asymmetric and symmetric stretching vibrations of the NO2 group at 1570-1485 cm^{-1} and 1370-1320 cm^{-1} ,respectively.[24] In this study, the asymmetric stretching mode of nitro group for 2B1F4NB is identified at 1674,1582 cm^{-1} in FTIR and 1382 cm^{-1} in FT-Raman spectrum with very strong intensity. Here one vibrational mode is slightly greater than the characteristic region and that may be affected due to the change in position of the nitro group.The bending ONO stretching modes are identified at 839 cm^{-1}.On the other hand, the calculated wave numbers at 1644,1584 and 1369 cm^{-1} is assigned to antisymmetric NO$_2$ stretching modes based on PED calculations.

The deformation vibrations of NO$_2$ group (rocking, wagging and to several normal modes) are in the low frequency region. [25] These bands were also found within the characteristic region and summarized in **Table.2.** The twisting modes of NO$_2$ in 2B1F4NB are identified in their characteristic regions and are presented in **Table.2.**The twisting modes of 2B1F4NB observed at 741,547cm^{-1} in FTIR and 326, 181 and 80cm^{-1} in FT Raman respectively.

5.2.5. C-X Vibrations: (C-X;X=Br, F)

Most aromatic bromo compounds absorb strongly in the region 650-395 cm^{-1} due to C Br stretching vibrations, although when there is more than one bromine atoms on the same carbon atom. The CBr stretching vibration is assigned to the strong mode 1040, 475cm^{-1} in FTIR and 231,298cm^{-1} and 691cm^{-1} FT Raman spectra, respectively.

The in-plane C-Br bending modes are observed at 475 cm^{-1} in FTIR and 231 cm^{-1} in FT-Raman, while the out of plane bending modes is at 438 in FTIR and 181cm^{-1} in FT Raman. The normal coordinate calculations signifies that the CBr in-plane bending is mixed with bCF, bCNO, bCN, bring modes. Similarly the CBr out of plane bending vibrations is also considered as a mixed mode. The out of plane bending vibrations observed at 438 cm^{-1} and 181cm^{-1} in FT Raman respectively. Both the experimental and the theoretical values are found to be in good agreement.

Aromatic fluorine compounds give stretching bands in the region 1270-1100cm^{-1}. [26] The vibrations are easily affected by the adjacent atoms (or) groups. The bands are appeared at 1526, 1305, 839 in FTIR and 1471 cm^{-1} in FT-Raman for 2B1F4NB is assigned to C-F stretching vibration. The out of plane bending mode for CF stretching is observed at 887, 231cm^{-1} in FT Raman and 475, 689cm^{-1} in FTIR spectrum respectively.

5.2.6. Ring Vibration

For aromatic ring, some bands are observed below 700cm^{-1}. These bands are quite sensitive to change in nature and position of the substituents. [27-30] Although other bands depend mainly on the substitution and the number of substituents rather than on their chemical nature (or) mass, so that these latter vibrations, together with the out-of-plane vibrations of the ring hydrogen atoms are to a great degree helpful in deciding the position of substituent. Two bands usually observed are those due to the in-plane and out-of-plane deformation vibrations. The in-plane deformation is at higher frequency the out of plane vibration and is generally weak, they are often masked by other stronger absorption which may occur due to the substituent groups [31].

For 2B1F4NB, the ring vibrations are observed at 1614, 1117, 1040, 839 cm^{-1} in FTIR and 631, 358, 298 in FT Raman and their corresponding calculated values are 1611 ,1118,1043, 823 in FTIR and 631, 358, 298 in FT Raman respectively. Also the ring torsional deformation vibration of 2B1F4NB is observed at 438,547 and 689 in FTIR and 80,181,326 and 887 cm^{-1} in Raman respectively.

6. Homo-Lumo analysis

On a fundamental level, there are a few approaches to compute the excitation energies. The first and simplest method involves the difference between the highest occupied molecular orbital (HOMO) and the lowest unoccupied molecular orbital (LUMO) of a neutral system. The energy gap between HOMO and LUMO is a critical parameter in determining molecular electrical transport [32].Molecular orbitals (HOMO and LUMO) and their properties such as energy are very useful for physicists and chemists and are very important parameters for chemistry. This form relates to the frozen orbital approximation, as the ground state properties are used to calculate excitation values. The HOMO-LUMO energy gap for 2B4F1NB has been calculated using DFT/B3LYP 6-311++G** Basis Sets. The Eigen values of HOMO-LUMO energy gap reflect the chemical reactivity of the molecule. The atomic orbital compositions of the molecular orbitals are outlined in **Fig.4.** The computed energies and the energy gap is

HOMO energy = **- 7.770487 eV**
LUMO energy = **-3.214482 eV**
HOMO-LUMO energy gap = **4.556004702 eV**

The decrease in the HOMO and LUMO energy gap explains the eventual charge transfer interaction taking place within the molecule, due to the strong electron-accepting ability of the electron-acceptor group. It is worth noting that HOMOs have an overall π bonding character along with a considerable non-bonding character and LUMOs have an anti-bonding π* character. The strong charge transfer interaction is responsible for the bioactivity of the molecule. [33]
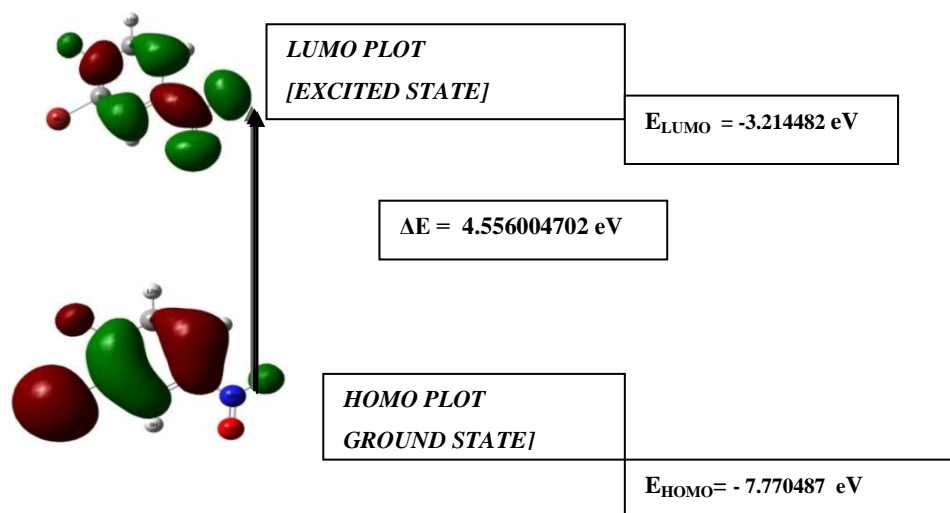

Fig.4.The atomic orbital compositions of the frontier molecular orbital (HOMO-LUMO) for 2B1F4NB

TABLE .4. *Energy values of 2B1F4NB by B3LYP/6 311++g(d,p) method*

Energies	Values
E_{HOMO} (eV)	- 7.770487 eV
E_{LUMO} (eV)	-3.214482 eV
E_{HOMO} - E_{LUMO} gap (eV)	4.556004 eV
Chemical hardness (η)	2.27800
Softness (S)	0.219490
Electronegativity (χ)	-5.49248
Chemical potential (μ)	5.49248
Electrophilicity index (ω)	6.6214575

Calculated value of electrophilicity index describes the biological activity. Every computed values of hardness, potential, softness and electrophilicity index are appeared in **Table.4.**

7.Analysis of Molecular Electrostatic Potential (MESP):

MESP values give understanding into the regions of a molecule which are more susceptible to electrophilic or nucleophilic attack. It gives information about the net electrostatic impact created by total charge distribution (electron + proton) of the molecule and relates with with dipole moments, electro-negativity, partial charges and chemical reactivity of the molecules. It gives a visual technique to understand the relative polarity of the molecule [34, 35].
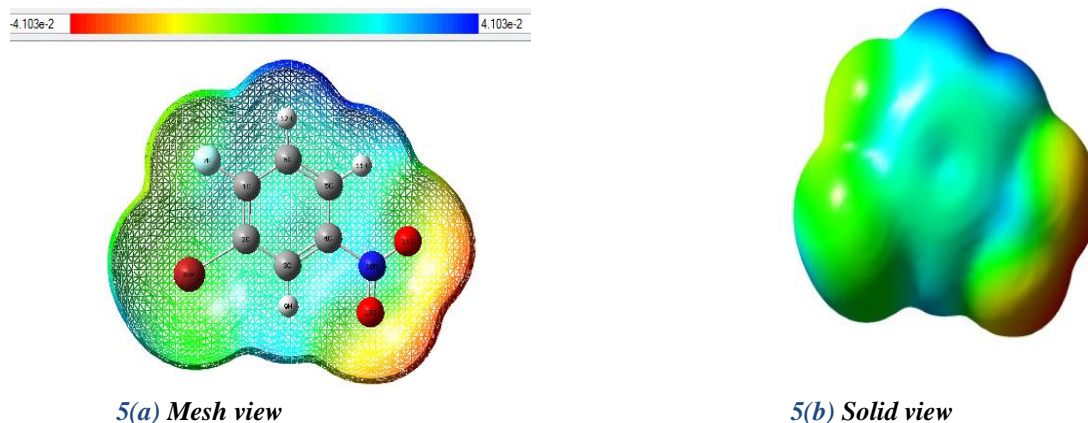.

| *5(a) Mesh view* | *5(b) Solid view* |

Fig.5.Electron density from total SCF density mapped with esp

An electron density iso-surface mapped with electrostatic potential surface portrays the size, shape, charge density and site of chemical reactivity of the molecules.
We can see the charge distributions of the molecule three dimensionally using Mesp map. Here the colour grading is very useful in research of molecular structure with its physiochemical property relationship. The different values of the electrostatic potential at the surface are represented by different colours. Red<orange<yellow<green<cyan<blue where blue (positive region) are related to nucleophilic reactivity. The regions of red shade represents the most negative electrostatic potential region and Green area covers parts of the molecule where electrostatic potentials are nearly equal to zero [36].
As can be seen from the MESP map of our present molecule, positive area are basically around the hydrogen atoms. The maximum negative area is restricted on the oxygen atoms of Nitro group. From the above **Fig.5.** regions having the negative potential are over the electronegative atoms, the region having the positive potential are over the hydrogen atoms and the remaining species are surrounded by almost equivalent to zero potential. The Electrostatic Potential from Total SCF Density mapped with esp is appeared in **Fig.5(a)** and **Fig.5(b)**.Also, the contour map of positive and negative potential for 2B1F4NB is appeared in **Fig.6.**
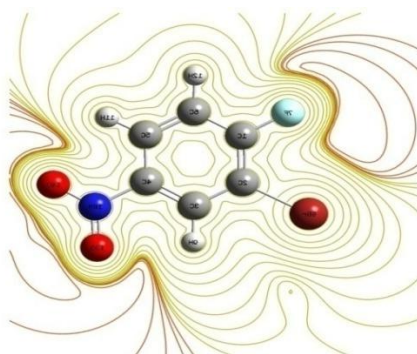
Fig.6.Contour Map of 2B1F4NB

8.Mulliken Analysis

The computation of nuclear charges assumes a critical part in the use of quantum mechanical calculations to molecular systems. The Mulliken atomic charge distribution has been used to describe the process of electronegativity equalization and model of electrostatic potential outside the molecular surface [37, 38]. Mulliken charges are calculated by determining the electron population of each atom as defined in the basis function.

The charge distribution on the molecule has an essential impact on the vibrational spectra. The corresponding Mulliken's plot with B3LYP/6-311++G (d,p) basis sets are appeared in **Fig.7.** The H9 atom has more positive charge than other hydrogen atoms. The carbon atom C2 is more positive than the other atoms due to electron donating substitution of that position. The total atomic charge of 2B1F4NB obtained by Mulliken population analysis with B3LYP basis sets were listed in **Table.5.** From the result it is clear that the substitution NO_2 atoms in the aromatic ring leads to a redistribution of electron density. The σ-electron withdrawing character of the nitrogen atom and Fluorine atom in 2B4F1NB is demonstrated by the decrease of electron density on C4 and C1 atoms. The C2 and C5 atoms are more acidic due to more positive charge. In addition, the histogram of Mulliken charges were shown in **Fig.8.**

Table.5. Atomic Charges for optimized geometry of 2B1F4NB using DFT-B3LYP/6-311++G(d,p)

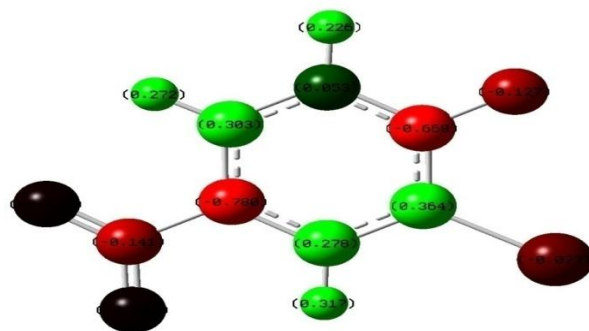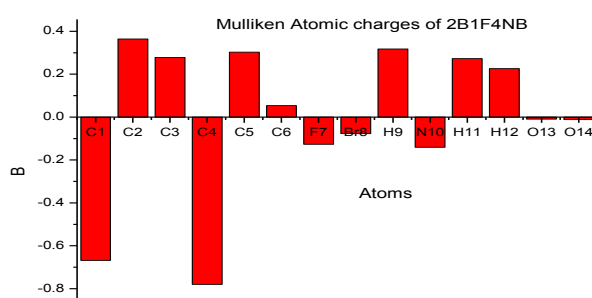| Atoms	Mullikken Atomic Charges
C1	-0.66799
C2	0.364311
C3	0.2778
C4	-0.78011
C5	0.303074
C6	0.05328
F7	-0.12654
Br8	-0.07706
H9	0.317308
N10	-0.14094
H11	0.272402
H12	0.225578
O13	-0.00911
O14	-0.01201

Fig.7. Mulliken atomic charges

Fig.8. Histogram of calculated Mulliken charges of 2B1F4NB

9. NBO Analysis

Natural bond analysis is started as a procedure for studying stability, bonding, intramolecular charge transfer (ICT) and donor- acceptor relationship. These all collectively contribute to determine the electronic structure property of the title compound 2B1F4NB.

Donor-Accpetor interactions:Perturbation theory energy analysis

NBO analyses of molecules delineate the deciphering of the molecular wave function as far as regularly comprehended by chemists: Lewis structures, charge, bond order, bond type, hybridisation, resonance, donor-acceptor interactions etc. The localised orbitals i the Lewis structure of 2B1F4NB can interact strongly. A filled bonding, antibonding or lone pair orbital can act as acceptor. These interactions can strengthen bond and weaken bonds. For example, a lone pair donor→antibonding acceptor orbital interaction will weaken the bond related with the antibonding orbital. On the other hand, an interaction with a bonding pair as the acceptor will strengthen the bond. Strong electron delocalisation in the Lewis structure likewise appears as donor-acceptor interactions. This calculation is done by examining all possible interactions between "filled" (donor) Lewis type NBOs and 'empty' (acceptor) non-Lewis NBOs and evaluating their energetic importance by second order perturbation theory. Since these interactions lead to loss of occupancy from the localised NBOs of the idealised Lewis structure into the empty non-Lewis orbitals (and thus, to departures from the idealised structure description),they are reffered to as delocalisation corrections to the natural Lewis structure.

The NBO technique shows the bonding concepts like atomic charge, Lewis structure, bond type, bond order, charge transfer and resonance possibility. Natural bond analysis is a useful tool for understanding delocalisation of electron density from occupied Lewis-type (donor) NBOs to properly unoccupied non-Lewis(acceptor)NBOs within the molecule. The stabilisation of orbital interaction is proportional to the interaction is proportional to the energy differerence between interacting orbitals. Therefore, the interaction having strongest stabilisation takes place between effective donors and effective acceptors. This bonding-antibonding interaction can be quantitatively described in terms of the NBO approach that is expressed by means of second order perturbation interaction energy $E^{(2)}$.[39-41]This stabilisation energy $E^{(2)}$ associated with i donor →j(acceptor) delocalisation is estimated from the second order perturbation approach[41] as given below

$$\mathbf{E^{(2)}} = \mathbf{qi}\,\frac{F^2(i.j))}{\epsilon_j - \epsilon_i}$$

Where qi is the donor orbital occupancy, ϵ_i and ϵ_j are diagonal elements (orbital energies) and F(i,j) is the off-diagonal Fock matrix element.

Here for our present compound, several types of electronic interactions available between bonding, non-bonding and anti-bonding orbitals. The prominent stabilization includes lone pair LP(3) to π^* and π to π^* transition in 2B1F4NB. The highest stabilization about 97.15 kJ mol^{-1} is observed at the interaction between LP(3) O14 $\rightarrow$ π^* (N10-O13). The $\pi \rightarrow \pi^*$ type of transition was observed at the interaction between C5$\rightarrow$ C6 and C1$\rightarrow$ C2 is about 25.35 kJ mol^{-1}. The atomic charges determined by natural bond orbital (NBO) analysis using B3LYP/6-311++G(d,p) method is presented in the **Table.6.**

Donor(i)	Type	ED/e	Acceptor(i)		ED/e	^{a}E(2) (KJ mol^{-1})	^{b}E(J)-E(i) (a.u.)	^{c}F(I,j) (a.u.)
C1-C2	σ	1.983	C1-C6	σ*	0.02878	4.18	1.27	0.065
			C2-C3	σ*	0.02325	2.96	1.29	0.055
C1-C2	π	1.64749	C3-C4	π*	0.38333	23.13	0.30	0.075
			C5-C6	π*	0.30048	15.22	0.31	0.062
C1-C6	σ	1.97576	C1-C2	σ*	0.04281	5.05	1.24	0.071
			C2-Br8	σ*	0.02872	4.79	0.81	0.056
			C5-C6	σ*	0.01309	2.22	1.27	0.048
			C5-H11	σ*	0.01234	1.86	1.20	0.042
			C6-H12	σ*	0.01132	1.20	1.18	0.034
C1-F7	σ	1.99517	C2-C3	σ*	0.02325	1.54	1.56	0.044
			C5-C6	σ*	0.01309	1.13	1.57	0.038
C2-C3	σ	1.97399	C1-C2	σ*	0.04281	2.88	1.25	0.05
			C1-F7	σ*	0.02971	3.57	0.99	0.053
			C3-C4	σ*	0.02436	3.52	1.27	0.060
			C4-N10	σ*	0.09429	3.97	1.03	0.058
C2-Br8	σ	1.98049	C3-C4	σ*	0.02436	3.27	1.19	0.056
C3-C4	σ	1.96824	C2-Br8	σ*	0.02872	4.55	0.81	0.054
C3-C4	π	1.64812	C1-C2	π*	0.41701	17.00	0.27	0.061
			C5-C6	π*	0.30048	21.78	0.29	0.071
			N10-O13	π*	0.5775	22.77	0.17	0.059
C3-H9	σ	1.97383	C1-C2	σ*	0.0428	4.40	1.05	0.061
			C4-C5	σ*	0.0218	4.20	1.07	0.060
C4-C5	σ	1.97707	C3-C4	σ*	0.02436	4.56	1.25	0.068
C5-C6	σ	1.97132	C4-N10	σ*	0.09429	4.52	1.00	0.061
	л	1.66262	C1-C2	л*	0.04170	25.35	0.26	0.074
	л		C3-C4	л*	0.38333	18.20	0.27	0.064
C5-H11	σ	1.97551	C3-C4	σ*	0.02436	4.59	1.06	0.062
C6-H12	σ	1.97489	C1-C2	σ*	0.04281	3.88	1.05	0.057
			C4-C5	σ*	0.02183	3.93	1.07	0.058
N10-O13	л	1.98654	C3-C4	л*	0.38333	3.55	0.47	0.040
	л		N10-O13	л*	0.57551	4.02	0.35	0.040
F7	LP(2)	1.96932	C1-C6	σ*	0.02878	6.06	0.94	0.068
F7	LP(3)	1.91099	C1-C2	л*	0.41701	20.84	0.41	0.090
Br8	LP(3)	1.92978	C1-C2	л*	0.41701	10.45	0.28	0.053
O13	LP(2)	1.87140	C4-N10	σ*	0.09429	14.50	0.58	0.083
O13	LP(2)		N10-O14	σ*	0.08438	24.82	0.54	0.104
O14	LP(2)	1.93470	C4-N10	σ*	0.09429	7.73	0.55	0.058
O14	LP(2)		N10-O13	σ*	0.03482	10.18	0.75	0.079
O14	LP(3)		N10-O13	л*	0.57551	97.15	0.13	0.104

Table.6. *Second order perturbation theory analysis of Fock matrix in NBO basis for 2B1F4NB*

[a]$E^{(2)}$ means energy of hyper conjugative interaction (stabilization energy)
[b]Energy difference between donor and acceptor i and j NBO orbitals.
[c]F(i,j) is the Fock matrix element between i and j NBO orbitals

10.HYPERPOLARIZABILITY

The first hyperpolarizability(β) of this novel molecular system of 2B1F4NB are calculated   utilizing B3LYP/6-311++G(d,p) basis set, based on the finite field approach. In the presence of an applied electric field, the energy of a system is a function of the electric field. First hyperpolarizability is a third rank tensor that can be described by a 3×3×3 matrix. The 27 components of the 3D matrix can be reduced to 10 components due to the Kleinman symmetry [42].It can be given in the lower tetrahedral format. It is clear that the lower part of the 3×3×3 matrices is a tetrahedral.

The polarizability and hyperpolarizability tensors (α_{xx}, α_{xy}, α_{yy}, α_{xz}, α_{yz}, α_{zz} and β_{xxx} ,β_{xxy}, β_{xyy}, β_{yyy}, β_{xxz}, β_{xyz} ,β_{yyz}, β_{zzz}) can be obtained by a frequency job output file of Gaussian. The mean polarizability (α_{tot}), anisotropy of polarizability ($\Delta\alpha$) and the average value of the first order hyperpolarizbilities (β_{tot})can be calculated using the equations.

$$\alpha_{tot} = \alpha_{xx} + \alpha_{yy} + \alpha_{zz/3}$$
$$\frac{1}{\sqrt{2}}[(\alpha_{xx} - \alpha_{yy})^2 + (\alpha_{yy} - \alpha_{zz})^2 + (\alpha_{zz} - \alpha_{xx})^2 + 6\,\alpha^2_{xx}]^{1/2}$$

The components of β are characterized as the coefficients in the Taylor series expansion of the energy in the external electric field. When the external electric field is weak and homogeneous, the expansion becomes:

$$\beta_{tot} = [(\beta_{xxx} + \beta_{xyy} + \beta_{xzz})^2 + (\beta_{yyy} + \beta_{xxy} + \beta_{yzz})^2 + (\beta_{zzz} + \beta_{xxz} + \beta_{yyz})2]^{1/2} \text{ and}$$
$$\beta_x = \beta_{xxx} + \beta_{xyy} + \beta_{xzz}$$
$$\beta_y = \beta_{yyy} + \beta_{yxx} + \beta_{yzz}$$
$$\beta_z = \beta_{zzz} + \beta_{zxx} + \beta_{zyy}$$
$$\beta_{tot} = [(\beta_x)^2 + (\beta_y)^2 + (\beta_z)^2]^{1/2}$$

The components of polarizability and the first hyperpolarizability of the title compound can be seen in **Table.7.**The first hyperpolarizability of the title compound is $1.451 10^{-30}$ esu which is 3.8921 times greater than those of urea(β of urea is 0.3728×10^{-30} esu).The calculated estimation of first hyperpolarizability demonstrates that 2B1F4NB may have the NLO properties.

Table.7. The Calculated Electric dipole moment , Polarizability and First Hyperpolarizability of 2B1F4NB

Dipole Moment μ		Polarizability α			First order Hyperpolarizability β		
Parameter	value	Parameter	a.u	esu($\times 10^{-24}$)	Parameter	a.u	esu ($\times 10^{-33}$)
μ_x	1.8317	α_{xx}	-90.8157	13.459	β_{xxx}	140.5978	1214.6
μ_y	2.2172	α_{xy}	-9.6255	1.4265	β_{xxy}	4.6357	40.048
μ_z	0.0002	α_{yy}	-71.5119	1.0598	β_{xyy}	22.5203	194.55
μ_{tot}	2.8759	α_{xz}	-0.0008	0.0001	β_{yyy}	1.1846	10.234
		α_{yz}	-0.0001	0	β_{xxz}	0.0027	2.3325
		α_{zz}	-74.3287	11.016	β_{yyz}	0.0000	0
		α_{tot}	78.89853	11.6928	β_{xzz}	18.4987	159.81
					β_{yzz}	-8.9425	77.254
					β_{zzz}	-0.0007	0.00604
					β_{xyz}	0.0006	0.005
					β	168.0298	1451.6
First order Hyperpolarizability β						$1.451 10^{-30}$ esu	

11.UV-Vis spectral analysis

The time–dependent density functional theory (TD-DFT) calculation has been performed for 2B1F4NB on the basis of fully optimized ground state structure to investigate the electronic absorption properties. This method is able to detect accurate absorption wavelengths at a relatively small computing time. Calculations of the molecular orbital geometry demonstrate that the visible absorption maxima of the molecule relate to the electronic transition between frontier orbitals such as transition from HOMO-LUMO.[43] The   values are obtained from the UV-Vis spectra analyzed theoretically with B3LYP/6-311G** Basis set. The UV-Vis spectrum is shown in **Fig.9.**

Electronic transitions are usually classified according to the orbitals connected with or to particular parts of the molecule involved. The λ_{max} is a function of substitution, the stronger the donor character substitution, the more electrons pushed into the molecules, the larger λ_{max}.[44] The theoretical electronic excitation energies, oscillator strengths and wavelength of the excitations were calculated and exhibited in Table.8.
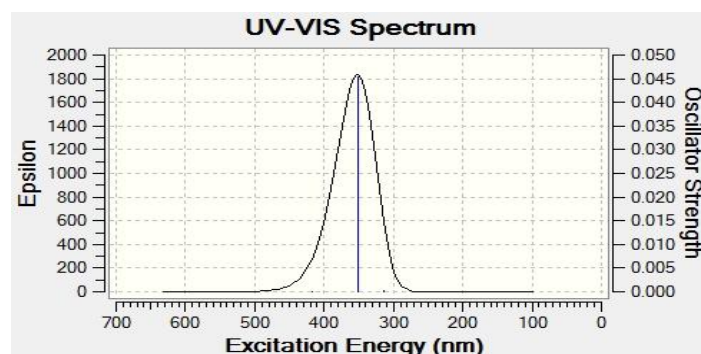
Fig.9. The UV-Visible Spectrum and excitation energy v/s oscillator strength of 2B1F4NB

Table.8.Theoretical electronic absorption spectra values of 2B1F4NB

Excited State	Energy (eV)	Wavelength λ (nm)	Oscillator strengths (f)
1	2.9751	416.74	0.0011
2	3.5229	351.94	0.0453
3	3.9579	313.26	0.0002

12. NMR spectroscopy

NMR spectroscopy is at present utilized for structure of organic molecules. The consolidated utilization of experimental and computer simulation methods offer a capable approach to interpret and predict the structure of large molecules. The optimized structure of 2B1F4NB was used to figure the NMR spectra at the DFT/B3LYP techniques with 6-311++G (d,p) level utilizing the GIAO method. [45] The theoretical ^{1}H and ^{13}C NMR chemical shifts of 2B1F4NB have been compared with the experimental data as shown in Table.9. Chemical shifts are reported for 2B1F4NB in ppm with respect to TMS for ^{1}H and^{13}C NMR spectra The theoretically calculated ^{13}C and ^{1}H NMR range are appeared in *Fig.10*.
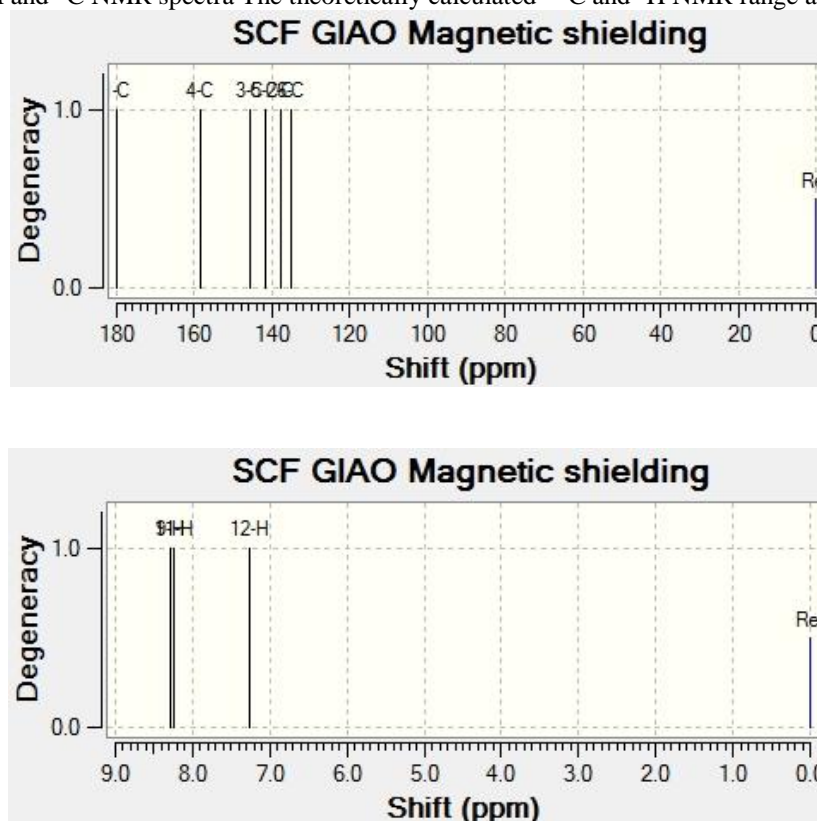

Fig.10.Theoretically calculated NMR spectrum of ^{1}H and ^{13}C for 2B1F4NB

Table.9. *Theoretically calculated NMR spectra of ^{1}H and ^{13}C 2B1F4NB*

Atom	Chemical Shift(ppm)
C1	179.9139
C2	137.8497
C3	145.5584
C4	158.5437
C5	141.7559
H9	8.2933000000
H11	8.2387000000
H12	7.2595000000

13.Thermodynamic Properties

In order to understand the thermodynamic behaviour of the present compound, the thermodynamic parameters(such as zero point vibrational energy, thermal energy, specific heat capacity, rotational constants, entropy and dipole moment) of 2B1F4NB are calculated by DFT/B3LYP method utilizing 6-311++G** basis sets at 298.15 K and 1 atm pressure and presented in Table.10. These functions depicts the thermodynamic stability of system at given conditions of pressure and temperature [46].It can be observed that these thermodynamic functions are increasing with temperature ranging from 100 to 1000 K due to the fact that molecular vibrational intensities increase with temperature.

All thermodynamic data give valuable formation for further studies. They can be used to compute other thermodynamic energies according to relationships of thermodynamic functions and estimate directions of chemical reactions according to the second law of thermodynamics in thermo chemical field. [47]

Table.10.*The Temperature dependence of Thermodynamic parameters of 2B1F4NB*

Temperature [T]	Energy[E] (KCal/Mol)	Heat capacity[Cv] (Cal/Mol-kelvin)	Entropy[s] (Cal/Mol-kelvin)
100	48.126	15.916	72.585
200	50.245	26.436	88.232
300	53.323	36.068	101.417
400	57.436	44.377	113.809
500	62.203	50.669	124.863
600	67.519	55.438	134.905
700	73.253	59.087	144.043
800	79.310	61.933	152.392
900	85.620	64.194	160.056
1000	92.134	66.019	167.127

The graph showing the correlation of heat capacity at constant pressure (Cp),entropy(S) and enthalpy change ($\Delta H0 \rightarrow T$) with temperature is delineated in **Fig.4** , **Fig.5** and **Fig .6.**
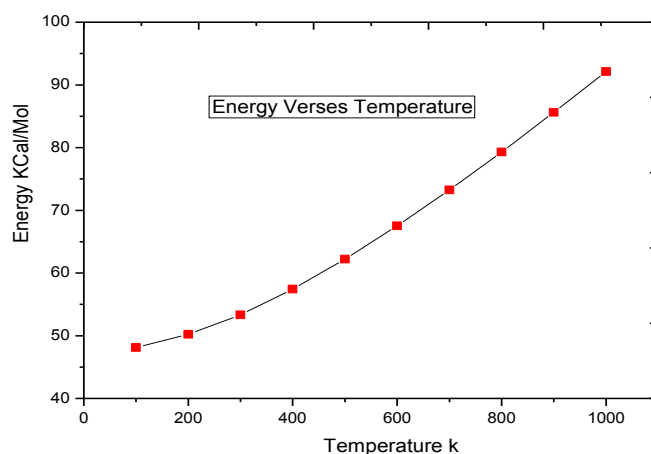

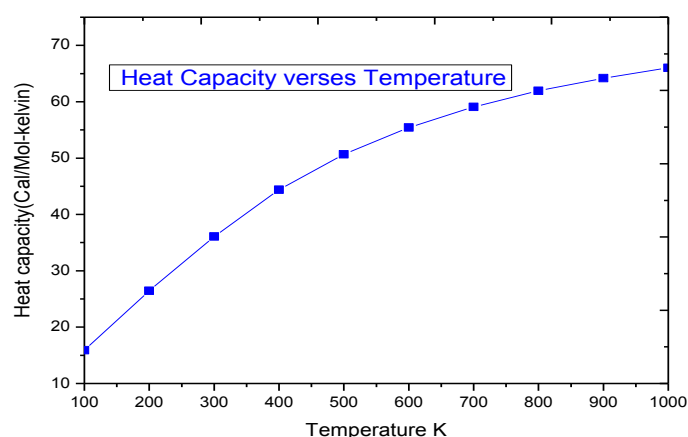*Fig.11. Temperature dependence of energy of 2B1F4NB*

Fig.12.Temperature dependence of Heat capacity at Constant Volume of 2B1F4NB
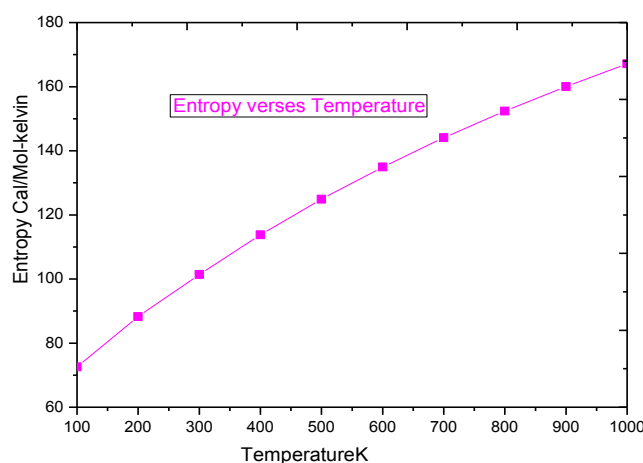

Fig.13. Temperature dependence of Entropy of 2B1F4NB

TABLE 11.The calculated Thermodynamical parameters of 2B1F4NB

Parameters	B3LYP/6-31G(d,p)
Zero-point vibrational energy (Kcal/Mol)	52.72494
Rotational constants (GHz):	A 1.48986
	B 0.45582
	C 0.34903
Dipole Moment	2.8760 Debye

V.CONCLUSION

In this study, the optimized molecular structure, PED, thermodynamic and electronic properties of the title compound are calculated by DFT method using B3LYP/6-311G (d,p)basis set. The complete molecular structural parameters and thermodynamics and temperature are also obtained .It was seen that the entropies increase with the increase in temperature as the intensities are enhanced by the higher temperature values. The fundamental vibrational modes o the title compound have been precisely assigned, analyzed and the experimental results were compared with the theoretical values. The influences of electronegative atoms on the atomic charges were studied in detail. The prediction of reactive behaviour of 2B1F4NB in both electophilic and nucleophilic reactions has been done with the help of MESP visualization. The chemical shift shielding tensors are predicted by the computational NMR method. The NBO analyses confirms the presence of resonance structures and reveals the exact s and p character of each bond. In 2B1F4NB molecules, the lone pair and the anti-bonding orbital is seen to give a strong stabilisation. The values of the energy separations between the HOMOs and LUMOs give significant information about these compounds. The dipole moment and hyperpolarizability result indicates the title molecule may have NLO property. Also, theoretical UV-Visible

spectrum was recorded. . Thus, the complete vibrational assignments, structural information and electronic properties of the title compound were provided in the present investigation.

REFERENCE

[1] B.A.Hess Jr.,L.J.Schaad,P.Carsky,andR.Zaharaduik, Chemical Reviews, vol.86, no.4, pp.709-730, 1986.

[2] P.Pulay,X.Zhou,and Forgarasi,in Recent Experimental and Computational Advances in Molecular Spectroscopy, R.Fausto and R.Fransto,Eds.,vol.406 of NATO ASI Series,p.99,Kluwer,Dordrecht, Netherlands,1993.

[3] P.Pulay,G.Forgarasi,G.Pongor,J.E.Boggs and A.Vargha, Journal of the American Chemical Society,vol.105,no.24,pp.7037-7047,1983.

[4] C.E.Blom and C.Altona,Molecular Physics,vol.31,no.5,pp.1377-1391,1976.

[5] G.Forgarasi and P.Pulay ,in Vibrational Spectra and structure,J.R.Durig,Ed.,Vol.14,Elsevier,Asterdam,Netherlands,1985.

[6] G.Forgarasi, Spectrochimica Acta A,vol.53,no.8,pp.1416,1997.

[7] G.R.de Mare,N.Yu.Panchenko, and W.Ch.Block,The Journal of Physical chemistry,vol.98,no.5,pp.1416-1420,1994.

[8] G.Pongor,P.Pulay,G.Forgarasi,and J.E.Boggs,"Theoretical prediction of vibrational spectra of pyridine,"Journal of the American Chemical Society,vol.106,no.10,pp2765-2769,1984.

[9] Y.Yamakitu and Tasumi,The Journal of Physical Chemistry,vol.99,no.2,pp.8524-8534,1995.

[10] M.Karaback,A.Coruh,adM.Kurt,Journal of Molecular Structure, Vol.892,no1-3,pp.125-131,2008.

[11] Peterson GA,Allaham MA(1991) J Chem Phys 94:6081-6090.

[12] Petersson GA,Bennett A,Tensfeldt TG,Allaham MA,Shirley WA,et al. (1988) J Chem Phys 89:2193-2218.

[13] Jamroz MH (2004) Vibrational Energy Distribution Analysis VEDA 4,Warsaw.

[14] Scott AP, Random L(1996) J Phys Chem 10016502-16504.

[15] G. Socrates, Infrared and Raman Characteristic group frequencies, Tables and Charts, third ed., Wiley, Chichester, 2001.

[16] Prabhavathi, A.Nilufer , V.Krishnakumar Spectrochem. Acta Part A Mol. Biomol. Spectrosc. .114(2013) 101-113.

[17] Socrates G, Infrared characteristic Group frequencies, 1st Ed, John Wiley, (1980).

[18] Colthup N B, Daly L H & Wiberly S E, Introduction to Infrared and Raman Spectroscopy, 2nd Ed (Academic Press, New York), 1975.

[19] Jag Mohan, Organic Spectroscopy—Principles and Applications, second ed., Narosa Publishing House, NewDelhi, 2001.

[20] J.Mohan,Organic Spectroscopy,Principle and Applications, Second ed., New Age International (P) Limted Publishers,New Delhi,2001.

[21] George Socrates, Infrared and Raman Characteristics Group Frequencies – Tables and Charts, third ed., John Wiley and Sons, New York, 2001

[22] N. Prabavathi et al. / Spectrochimica Acta Part A: Molecular and Biomolecular Spectroscopy 96 (2012) 226–241.

[23] S.Seshadri, Rasheed .M.P International Journal of Engineering And Science Vol.6, Issue 4 (April 2016), PP - 06-18.

[24] N.Sundaraganesana, S.Ayyappana, H.Umamaheswari B. Dominic Joshua,Spectrochimica Acta Part A 66 (2007) 17–27.

[25] P.S. Peek, D.P. Mcdermoot, Spectrochim. Acta 44 (1988) 371–377.

[26] Bakiler M, Maslov I V & Akyiiz S, J Mol Struct, 475 (1999) 83.

[27] R.J. Jakobsen, F.F. Bentley, Appl. Spectrosc. 18 (1964) 82–88.

[28] A. Mansingh, J. Chem. Phys. 52 (1970) 5896–5902.

[29] L. Verdonck, G.P. Vander Kelen, Z. Eeckhant, Spectrochim. Acta Part A 29 (1973) 813–816.

[30] L. Verdonck, G.P. Vander Kelen, Spectrochim. Acta Part A 28 (1972) 55–57.

[31] N.Prabavathi et al.Spectrochimica Acta Part A: Molecular and Biomolecular Spectroscopy 96 (2012) 226–241 241.

[32] S.Seshadri , Rasheed .M.P & R.Sangeetha IOSR Journal of Applied Chemistry, Volume 8, Issue 8 Ver. II (Aug. 2015), PP 87-100.

[33] [33]D.M. Suresh, M. Amalanathan˙S. Sebastian, D. Sajan, I. Hubert Joe, V. Bena Jothy, Ivan Nemec, Spectrochimica Acta Part A: Molecular and Biomolecular Spectroscopy Volume 115, November 2013, Pages 595–602

[34] S. Chidangil, M.K. Shukla, P.C. Mishra, J. Mol. Model. 4 (1998) 250–258.

[35] F.J. Luque, J.M. Lopez, M. Orozco, Theor. Chem. Acc. 103 (2000) 343–345. [37]

[36] M.Raja et.al/Journal of Molecular Structure,1141(2017) 284-298.

[37] K. Jug, Z.B. Maksic, in: Z.B. Maksic (Ed.), Theoretical Model of Chemical Bonding, Part 3, Springer, Berlin, 1991, p. 233.

[38] S. Fliszar, Charge Distributions and Chemical Effects, Springer, New York, 1983.

[39] A.E. Reed, R.B. Weinstock, F. Weinhold, J. Chem. Phys. 83 (1985) 735–746.

[40] A.E. Reed, F. Weinhold, J. Chem. Phys. 78 (1983) 4066–4073.

[41] J.P. Foster, F. Weinhold, J. Am. Chem. Soc. 102 (1980) 7211–7218. [46]

[42] R.N. Singh, Amit Kumar, R.K. Tiwari, Poonam Rawat, Vikas Baboo, Divya Verma, Spectrochimica Acta Part A 92 (2012) 295– 304.

[43] S.Seshadri, R.Sangeetha , Rasheed .M.P, M.Padmavathy (International Research Journal of Engineering and Technology (IRJET), Volume: 03 Issue: 10 Oct -2016.

[44] N. Subramanian, N. Sundaraganesan, J. Jayabharathi, Spectrochim. Acta A 76 (2010) 259 - 269.

[45] S.Seshadri, Rasheed .M.P, R.Sangeetha, IOSR Journal of Applied Physics, Volume 7, Issue 6 Ver. I (Nov. - Dec. 2015), PP 56-70.

[46] Ran Z, Baotong D, Gang S and Yuxi S *Spectrochim Acta Part A* **75** (2010) 1115

[47] J.B. Ott, J.B. Goates, Chemical Thermodynamics: Principles and Applications, Academic San Diego, 2000.